A unique case of inflammatory myofibroblastic tumor of the liver manifesting with biloma: A case report

KUN HUANG[1], PINGWU ZHAO[1], JIANGYING ZHAO[2], PAN ZHAO[1] and JIAN YANG[3]

Departments of [1]General Surgery and [2]Pathology, Mianyang Hospital of Traditional Chinese Medicine, Mianyang, Sichuan 621000; [3]Department of Liver Surgery, West China Hospital, Sichuan University, Chengdu, Sichuan 610000, P.R. China

Received December 24, 2021; Accepted April 22, 2022

DOI: 10.3892/ol.2022.13348

Abstract. Anaplastic lymphoma kinase (ALK)-negative hepatic inflammatory myofibroblastic tumors (IMTs) harboring the ETS variant transcription factor 6-neurotrophic receptor tyrosine kinase 3 (*ETV6-NTRK3*) fusion gene and manifesting with biloma are extremely rare, and their biological behavior is unclear. The present study reports the case of a 45-year-old female with ALK-negative IMT of the liver harboring the *ETV6-NTRK3* fusion gene and manifesting with biloma. Computed tomography of the abdomen confirmed the lesions to be a low-density mass, measuring 11.2x8.5x10.5 cm, located in the left lobe of the liver, and a lower-density mass, measuring 8.5x6.1x5.9 cm, located in the interior of the tumor. As the suspicion of a malignancy remained high, surgical resection of the left hepatic lobe, including the tumor, was undertaken. Intraoperatively, a tumor (12x10x9 cm), with an unclear boundary, incomplete capsule and fish-like texture, was found in the left lateral lobe of the liver, and a biloma, measuring 8x6 cm, was identified inside the tumor. Pathological examination revealed spindle cell proliferation with infiltration of chronic inflammatory cells and mucinous degeneration. Immunohistochemical studies showed negativity for ALK, CD117, CD34, discovered on GIST-1, desmin, smooth muscle actin, S-100, CD21, pan-cytokeratin, epithelial membrane antigen, CD23 and CD35, but positivity for vimentin staining, and 5% Ki-67-positive cells. Fluorescence *in situ* hybridization studies assessing characteristic genetic rearrangements using *ALK, RET, ROS1, MDM2, MGEA5* and *ETV6* break-apart assays, revealed the presence of the *ETV6-NTRK3* fusion oncogene and negativity for *ALK, RET, ROS1*, *MDM2* and *MGEA5*. The patient was discharged 7 days post-operatively, without any adjuvant treatment. No recurrence of symptoms was noted at the 3-year follow-up. To the best of our knowledge, this is the first report of biloma in an ALK-negative IMT of the liver, which may increase our understanding of hepatic IMT.

Correspondence to: Professor Jian Yang, Department of Liver Surgery, West China Hospital, Sichuan University, 37 Guo Xue Lane, Chengdu, Sichuan 610000, P.R. China
E-mail: yangjian19820810@hotmail.com

Key words: hepatic inflammatory myofibroblastic tumor, *ETV6-NTRK3* fusion gene, anaplastic lymphoma kinase, biloma

Introduction

An inflammatory myofibroblastic tumor (IMT) is a borderline tumor with low malignant potential (1,2), comprised of spindle cells and accompanied by an inflammatory infiltrate of plasma cells, lymphocytes and/or eosinophils (3,4). The lungs, abdominal cavity and gastrointestinal tract are common sites of IMT, but primary hepatic IMT is rare (5). The biological behavior of the tumor remains unclear (6). IMTs are usually benign, but sometimes, malignant biological behavior such as distant metastasis and local recurrence may occur (6,7). The anaplastic lymphoma kinase (*ALK*) gene, encoding a receptor tyrosine kinase belonging to the insulin receptor superfamily (8), has been found to be rearranged in ~50% of patients with IMT, which results in the overexpression and hyperactivation of the receptor tyrosine kinase (4,9). Therefore, ALK protein has important value in the diagnosis of IMT; for ALK-negative patients, the novel ETS variant transcription factor 6-neurotrophic receptor tyrosine kinase 3 (*ETV6-NTRK3)* fusion gene, has important reference value for diagnosis (4,10,11).

A biloma is a well-circumscribed intra-abdominal bile accumulation outside the biliary tree (12); it can either be intrahepatic or extrahepatic (12), with an incidence of 0.3-2% (13). The most common cause is choledocholithiasis, and other causes include abdominal trauma and surgery, bile duct tumors, liver infarction, percutaneous catheter drainage, transhepatic cholangiogram and endoscopic retrograde cholangiopancreatography, and fever, nausea, vomiting and epigastralgia are common symptoms caused by biloma (13).

To the best of our knowledge, there are no reported cases of hepatic IMT manifesting with biloma. The present study reports the case of a 45-year-old woman with hepatic IMT negative for ALK upon immunohistochemistry and fluorescence *in situ* hybridization (FISH) studies, in whom a biloma was identified inside the hepatic IMT.

Case report

In March 2019, a 45-year-old woman presented to Mianyang Hospital of Traditional Chinese Medicine (Mianyang, China)

with a solid, well-defined mass in the right upper quadrant of the abdomen. The patient had no abdominal pain, fever, vomiting or jaundice, and no history of hepatitis B or exposure to parasites. Laboratory data showed a white blood cell count, a red blood cell count and a platelet count of $5.17x10^9$/l (reference range, 3.5-$9.5x10^9$/l), $4.05x10^{12}$/l (reference range, 4.3-$5.8x10^{12}$/l) and $218x10^9$/l (reference range, 100-$300x10^9$/l), respectively, while neutrophil, lymphocyte, eosinophil and basophil levels were 59.9% (reference range, 50-70%), 32.3% (reference range, 20-40%), 1.0% (reference range, 0-7%) and 0.4% (reference range, 0-2%), respectively. Hemoglobin was recorded at 124 g/l (reference range, 120-170 g/l). Alanine aminotransferase, aspartate amino transferase, alkaline phosphatase, glutamyl transpeptidase and lactate dehydrogenase levels were 33 U/l (reference range, 0-50 U/l), 26.5 U/l (reference range, 0-40 U/l), 74.7 U/l (reference range, 45-125 U/l), 17.4 U/l (reference range, 10-60 U/l) and 145.0 U/l (reference range, 120-250 U/l), respectively. Total bilirubin, indirect bilirubin and direct bilirubin levels were 11.50 μmol/l (reference range, 3.42-20.5 μmol/l), 1.30 μmol/l (reference range, 0-6.84 μmol/l) and 10.20 μmol/l (reference range, 0-18 μmol/l), respectively. α-fetoprotein and carcinoembryonic antigen results were 3.21 μg/ml (reference range, 0-20 μg/ml) and 1.30 μg/ml (reference range, 0-5 μg/ml), and carbohydrate antigen 125 (CA125), CA153 and CA19-9 results were 7.50 KU/ml (reference range, 0-35 KU/ml), 10.60 KU/ml (reference range, 0-35 KU/ml) and 7.30 KU/ml (reference range, 0-35 KU/ml), respectively.

Computed tomography of the abdomen confirmed the presence of the lesion, revealing a low-density mass measuring 11.2x8.5x10.5 cm in the left lobe of the liver, with a lower-density mass measuring 8.5x6.1x5.9 cm in the interior of the tumor (Fig. 1A and B). Based on the analysis of patient history, laboratory data and imaging data, the characteristics of the lesion were different from hepatocelluar carcinoma, cholangiocarcinoma, intrahepatic cholangiocarcinoma, liver abscess and hepatic echinococcosis. Furthermore, IQQA-3D (EDDA Technology, Inc.) imaging of the neoplastic area was performed for precise preoperative evaluation (Fig. 2), and the lesion could be easily removed by radical resection. As suspicion of a malignancy remained high, surgical resection of the left hepatic lobe, including the tumor, was undertaken. Intraoperatively, a tumor (12x10x9 cm), with an unclear boundary, incomplete capsule and fish-like texture, was found in the left lateral lobe of the liver, and a biloma, measuring 8x6 cm, was identified inside the tumor (Fig. 1C). The resection margins were clear.

The histopathological review of the sections (4-μm-thick) was performed using hematoxylin and eosin staining. The tumor excision tissue was stored as wax blocks in routine storage at ambient temperature prior to staining. The fixation protocol involved the use of 10% neutral buffered formalin as the fixant, with the duration of fixation being 24 h at room temperature. Following dehydration in a series of ethanol solutions, the tumor excision tissues were paraffin-embedded and sliced into 4-μm-thick sections. Firstly, the sections were deparaffinized in xylene (10 min three times) and rehydrated by serial soaking in 100% ethanol for 10 min, and 95, 85 and 75% ethanol for 5 min each at 25˚C. Secondly, sections were stained in 0.1% hematoxylin solution (10 min at 25˚C) and differentiated in 1% hydrochloric alcohol, then rinsed with tap water and with distilled water until the nuclei became blue, and dehydrated in 95% ethanol. Thirdly, sections were counterstained in 0.5% eosin solution (3 min at 25˚C), and incubated in 95% anhydrous ethanol for 5 min twice and in xylene solution for 10 min at 25˚C. Lastly, the sections were sealed with Canada gum. Normal light microscopy was used to image the H&E staining at a magnification of x200. Spindle cell proliferation with infiltration of chronic inflammatory cells and mucinous degeneration were found (Fig. 3).

For immunostaining, the streptavidin-peroxidase method was adapted to detect protein expression using paraffin sections. The tumor excision tissue was stored as wax blocks in routine storage at room temperature. The fixation protocol involved the use of 10% neutral buffered formalin as the fixant, with the duration of fixation being 24 h at room temperature. Tissue sections (4-μm-thick) were dried at 60˚C for 2.5 h, deparaffinized with two 10-min washes in xylene, and rehydrated in decreasing concentrations of ethanol in distilled water (100, 95, 85 and 75%; 5 min each). Next, sections were soaked in boiling sodium citrate buffer (20140006; Henan Celnovte Biotechnology, Co., Ltd.) for 2.5 min in a microwave oven. When cooled to room temperature, the sections were washed for 5 min in distilled water two times and for 5 min in PBS (20140002; 0.01 M pH 7.2-7.4; Henan Celnovte Biotechnology, Co., Ltd.) one time. Subsequently, sections were treated with 3% hydrogen peroxide at room temperature for 5 min to block endogenous peroxidase activity. After washing for 5 min in PBS two times, the sections were incubated for 60 min at 18-25˚C with ALK (rat anti-human) antibody (202011001; clone 5A4; dilution, 1:100; Henan Celnovte Biotechnology, Co., Ltd.) and washed for 5 min in PBS two times, followed by incubation with HRP-labeled goat anti-rat IgG antibody (20170011; dilution, 1:100; Henan Celnovte Biotechnology, Co., Ltd.) for 20 min at 18-25˚C, washing with PBS for 5 min (two times), incubation for 3-5 min at 18-25˚C with diaminobenzidine (DAB; DAB substrate:DAB buffer=1:20; 20170011; Henan Celnovte Biotechnology, Co., Ltd.), washing for 5 min in distilled water two times, and counterstaining with 5% hematoxylin (20170011; Henan Celnovte Biotechnology, Co., Ltd.) for 5 min. Finally, the sections were stained blue in 1% hydrochloric-acid alcohol at room temperature, dehydrated in increasing concentrations of ethanol (85, 95 and 100%), cleared with xylene, and were sealed with Canada gum.

In order to ensure the accuracy and reliability of the staining conclusion, both positive control and negative control experiments were set up for each section to be detected according to the manufacturer's instructions during the experiment. A blank control was used as a negative control and an anaplastic lymphoma tissue section was used as a positive control. Analysis was performed using an Olympus BX 53 light microscope (magnification, x200; Olympus Corporation). The aforementioned steps were repeated for CD117 (clone EP10), CD34 (clone QBEnd/10 mouse), discovered on GIST-1 (clone RBT-DOG-1), desmin (clone EP15), smooth muscle actin (clone IA4), S-100 (clone poly), CD21 (clone EP64), pan-cytokeratin (clone AE1/AE3), epithelial membrane antigen (clone aP1.4), CD23 (clone, aR013), vimentin (clone V9) and CD35 (clone RLB25 mouse) (all Henan Celnovte Biotechnology, Co., Ltd.) according to the manufacturer's instructions for each antibody.

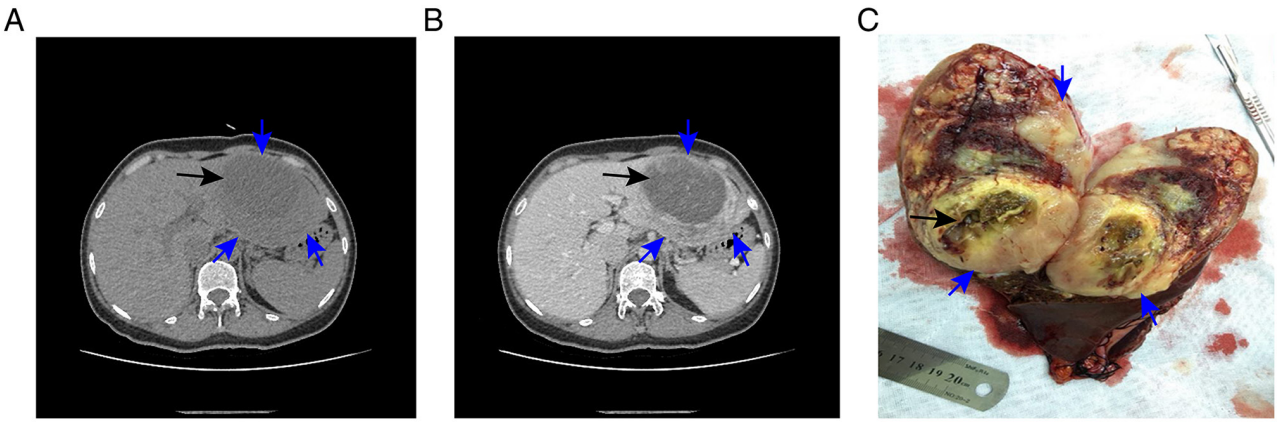

Figure 1. IMT upon abdominal computed tomography and its gross morphology. (A and B) IMT on abdominal computed tomography. (C) Gross morphology of the IMT. The blue arrows indicate the IMT and the black arrows indicate the biloma. IMT, inflammatory myofibroblastic tumor.

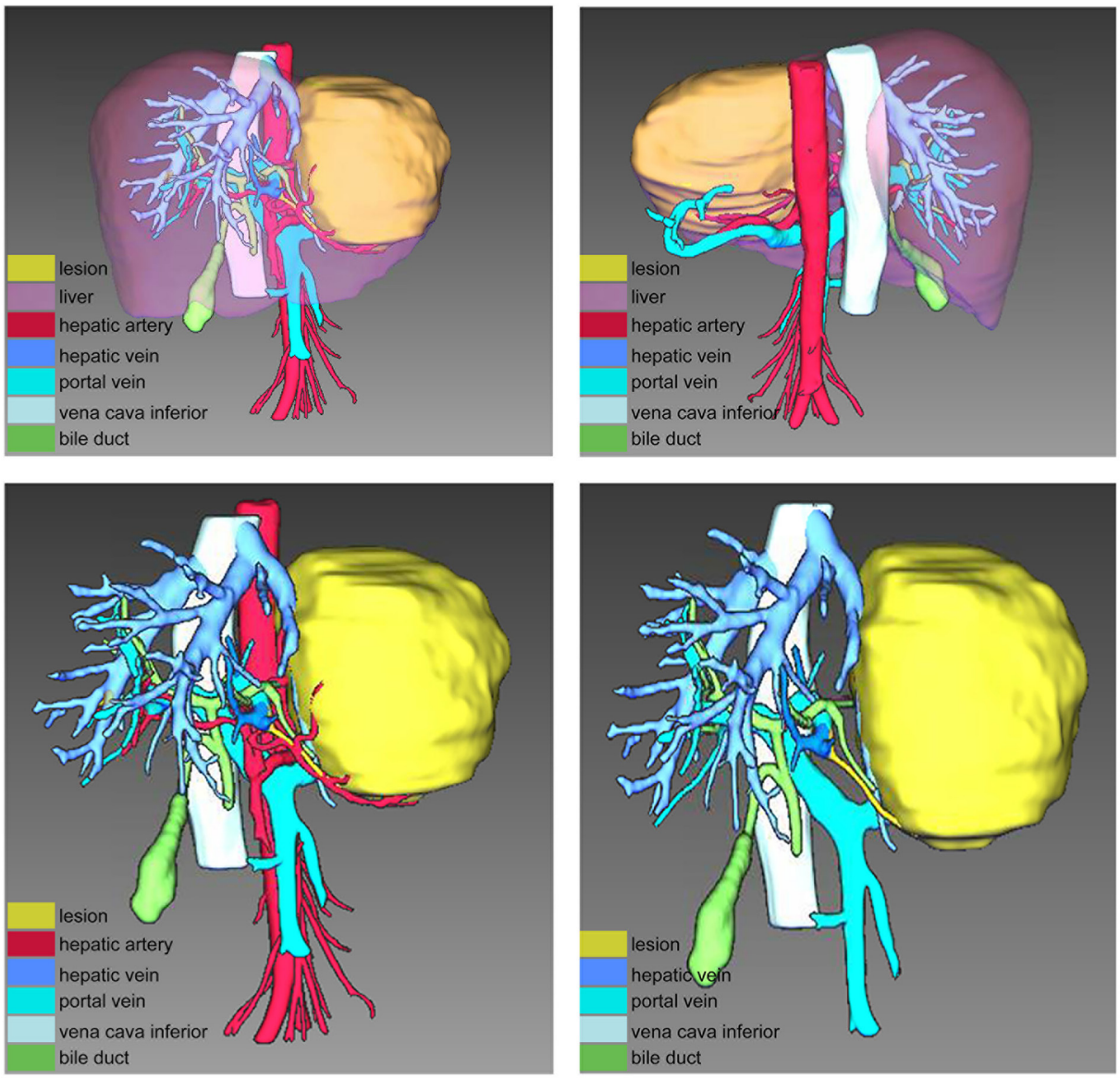

Figure 2. IQQA-3D (EDDA Technology, Inc.) imaging of the tumor.

This revealed negativity for ALK (clone 5A4), CD117 (clone EP10), CD34 (clone QBEnd/10 mouse), discovered on GIST-1 (clone RBT-DOG-1), desmin (clone EP15), smooth muscle actin (clone IA4), S-100 (clone poly), CD21 (clone EP64),

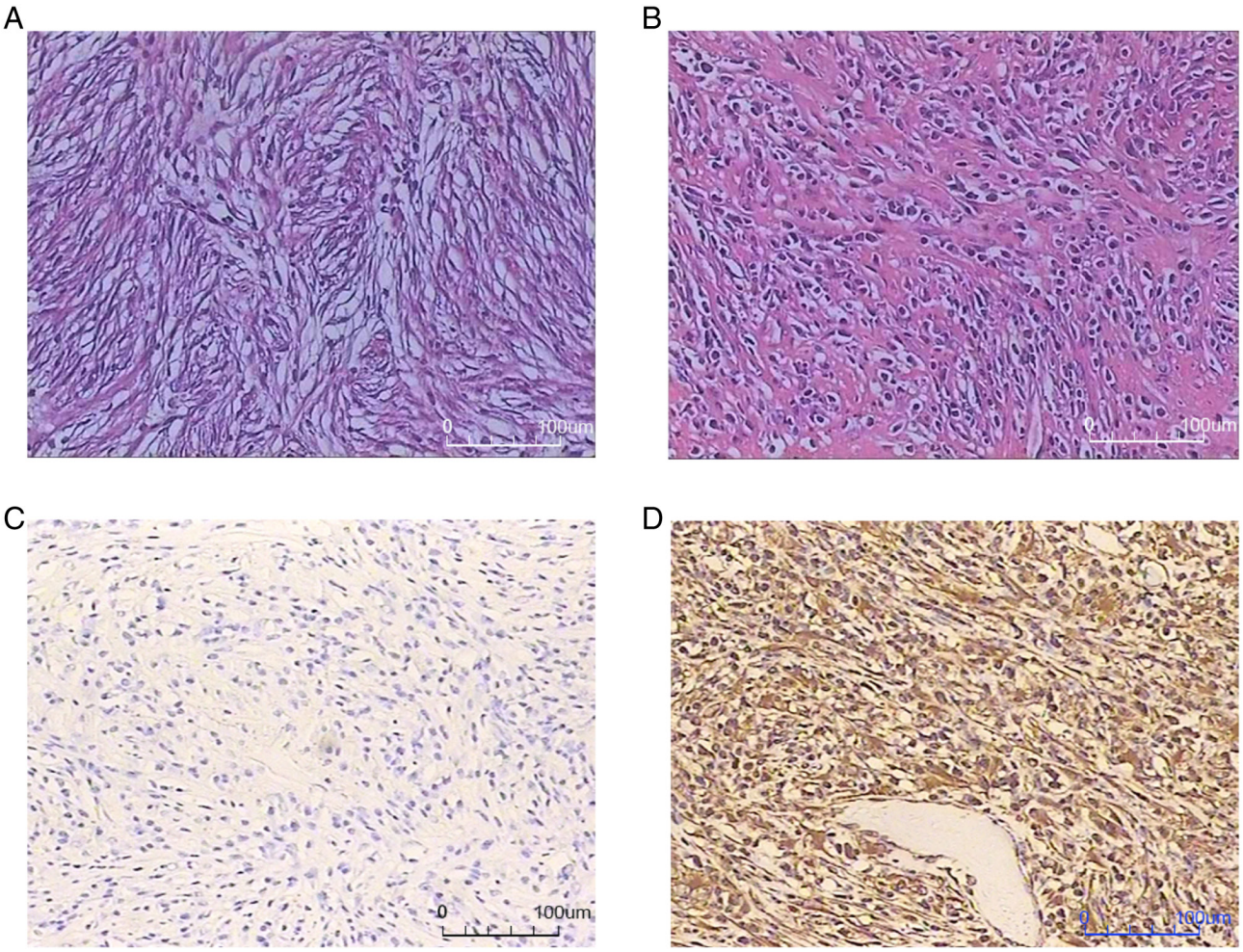

Figure 3. Hematoxylin and eosin staining, and immunohistochemistry. (A) Fibroblastic spindle cells and inflammatory infiltrate upon hematoxylin and eosin staining (magnification, x200). (B) Mucinous degeneration identified by hematoxylin and eosin staining (magnification, x200). (C) ALK detection by immunohistochemistry, showing a lack of staining (magnification, x200). (D) Positive vimentin detection by immunohistochemistry (magnification, x200).

pan-cytokeratin (clone AE1/AE3), epithelial membrane antigen (clone aP1.4), CD23 (clone, aR013) and CD35 (clone RLB25 mouse) (all Henan Celnovte Biotechnology, Co., Ltd.), and positive staining for vimentin (clone V9), with 5% Ki-67-positive cells (Fig. 3).

This phenotype is not typical of IMT (11). To confirm the diagnosis, FISH studies were conducted to assess characteristic genetic rearrangements using *ALK* (Fracture rearrangement probe; cat. no. F.01079; Guangzhou Anbiping Pharmaceutical Technology Co., Ltd.), *RET* (Fracture rearrangement probe; cat. no. F.01104-01; Guangzhou Anbiping Pharmaceutical Technology Co., Ltd.), *ROS1* (Fracture rearrangement probe; cat. no. F.01086; Guangzhou Anbiping Pharmaceutical Technology Co., Ltd.), *MDM2* (Fracture rearrangement probe; cat. no. F.01017-01; Guangzhou Anbiping Pharmaceutical Technology Co., Ltd.), *MGEA5* (Fracture rearrangement probe; cat. no. F.01275-01; Guangzhou Anbiping Pharmaceutical Technology Co., Ltd.) and *ETV6* break-apart assays (Fusion probe; cat. no. F.01258-01; Guangzhou Anbiping Pharmaceutical Technology Co., Ltd.). The tumor excision tissue was stored as wax blocks in routine storage at room temperature. The fixation protocol involved the use of 10% neutral buffered formalin as the fixant, with the duration of fixation being 24 h at room temperature. The tissues were embedded in paraffin. Corresponding H&E sections were reviewed by a pathologist who circled the area of tumor for testing.

ALK FISH was performed using 4-μm-thick FFPE tissue sections. Sections were deparaffinized, rehydrated in 100, 90 and 70% ethanol, washed with 2x saline sodium citrate (SSC) (UltraPure™ 20X SSC; Invitrogen; Thermo Fisher Scientific, Inc.), incubated in pretreatment solution (deionized water; 25 min at 90˚C), and digested with pepsin solution (1:10,000; Sigma-Aldrich; Merck KGaA; 4 mg/ml pepsin; 0.02 mol/l HCL) for 6 min at 37˚C. Subsequently, sections were washed with 2x SSC (5 min at room temperature), dehydrated in ethanol (70, 90 and 100%), dried at room temperature and then exposed to 10 μl *ALK* gene probe (Fracture rearrangement probe; cat. no. F.01079; batch number, 202110001; concentration, 60 ng/μl; Guangzhou Anbiping Pharmaceutical Technology Co., Ltd.). Denaturation (5 min at 85˚C) and hybridization (10-18 h at 37˚C) were performed using the ThermoBrite System (Abbott Pharmaceutical Co. Ltd.). After 24 h, the specimens were treated with 2x SSC (36 ml pure water + 4 ml 20X SSC) for 10 min at 37˚C, 2x SSC containing 0.1% Nonidet P-40 (NP 40; Nacalai Tesque Inc.; 36 ml pure

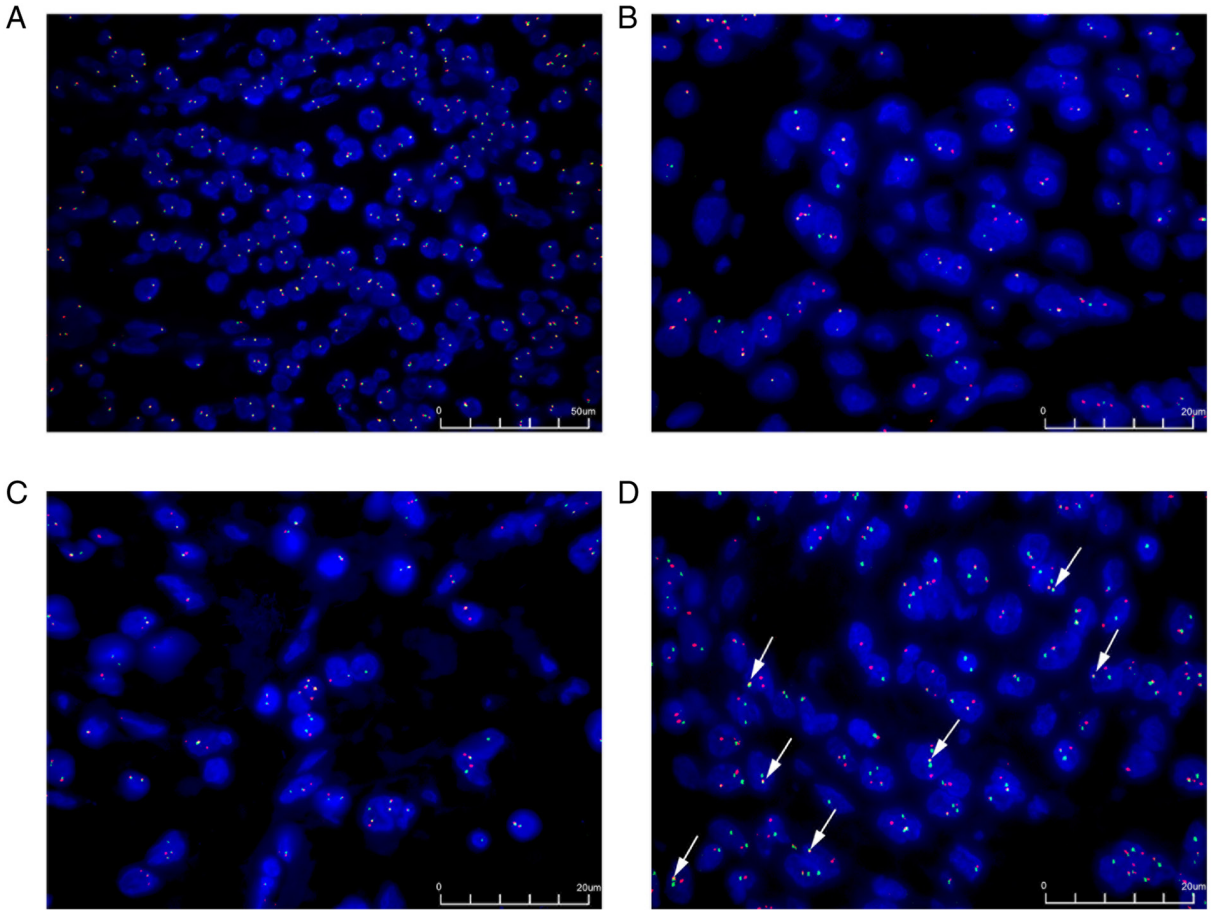

Figure 4. Fluorescence *in situ* hybridization. (A) The anaplastic lymphoma kinase gene was detected using a broken rearrangement probe. The proportion of positive cells was 3% (magnification, x400). (B) The *ETV6* gene was detected using a broken rearrangement probe. The green signal represents the GSP *ETV6* (centromere) and the red signal represents the GSP *ETV6* (telomere) (magnification, x1,000). (C) The *NTRK3* gene was detected using a broken rearrangement probe. The green signal represents the GSP *NTRK3* (telomere) and the red signal represents the GSP *NTRK3* (centromere) (magnification, x1,000). (D) The *ETV6-NTRK3* fusion gene was detected using the fusion gene probes. The white arrow shows the typical *ETV6-NTRK3* fusion gene, which is demonstrated by the close proximity of the red signal (*ETV6* from chromosome 12) with the green signal (*NTRK3* from chromosome 15) in multiple tumor cells. ETV6, ETS variant transcription factor 6; NTRK3, neurotrophic receptor tyrosine kinase 3 (magnification, x1,000). GSP, gene-specific primer.

water + 4 ml 20X SSC + 40 μl NP-40) for 5 min at 37˚C, rehydrated in 70% ethanol (3 min, at room temperature) and dried in the dark. Nuclei were counterstained with DAPI using antifade reagent for 30 min at -20˚C (VECTASHIELD Mounting Medium; Vector Laboratories, Inc.). Analysis was performed using a fluorescence microscope (magnification, x1,000; Axio imager Z1; Carl Zeiss AG) and data analysis was performed using ISIS software (version 5.4.6; MetaSystems). FISH signal was classified under two signal patterns: Normal (two yellow signals) and typical positive signal pattern (one red, one green and one yellow signal), and >100 tumor cells were assessed. The aforementioned steps were repeated for RET, ROS1, MDM2 and MGEA5 genes and ETV6-NTRK3 fusion genes according to the manufacturer's instructions for each gene. These studies found an *ETV6* rearrangement, identified as an *ETV6-NTRK3* fusion oncogene. *ALK, RET, ROS1, MDM2* and *MGEA5* were negative (Fig. 4).

Finally, a diagnosis of hepatic IMT with biloma was made, based on morphological and immunohistochemical findings, and the characteristic genetic rearrangements. The postoperative course was uneventful, and the patient was discharged at postoperative day 7. The patient was followed up every 3 months without adjuvant treatment. No recurrence of symptoms was noted at the 3-year follow-up and outpatient follow-up every 6 months will still be performed.

Discussion

According to the World Health Organization classification of soft-tissue tumors, IMT is a borderline tumor with low malignant potential; it is a mesenchymal neoplasm comprising myofibroblastic and fibroblastic spindle cells, accompanied by an inflammatory infiltrate of plasma cells, lymphocytes and/or eosinophils (4,5,14). The lung is the most common site of IMT (15). In addition, IMTs originating from female genital organs (4,16), the intra-abdominal region (17,18), the retroperitoneum (19), the ileocecal mesentery (20) and the pancreas (21) have also been reported. However, those located in the liver are even rarer (5).

The *ALK* gene was first discovered in 1994 in a subtype of anaplastic large cell lymphoma (22), located on chromosome 2p23, encoding ALK (22). Previous studies have confirmed that *ALK* gene rearrangements are found in nearly one-half of patients with IMT, which leads to *ALK* overexpression (4,11,23).

Therefore, the ALK protein is considered to be an important feature for identifying IMT (4).

For ALK-negative patients, recent studies have identified some new fusion genes, mainly including the *ROS1, ETV6, PDGFRβ, RET* and *NTRK3* genes (10,11,24). A case of ALK-negative uterine IMT harboring the *ETV6-NTRK3* fusion gene was reported by Takahashi *et al* (4). Alassiri *et al* (11) also found that *ETV6-NTRK3* is expressed in a subset of ALK-negative IMTs. These findings are consistent with the characteristic genetic rearrangements of the present patient.

The biological behavior of the tumor is an important factor affecting the prognosis of the patient, as well as an important reference for developing a treatment plan. However, the biological behavior of IMT is unclear. ALK is more commonly expressed in children and is associated with tumor aggressiveness and high recurrence rates (2). By comparison, ALK-negative IMT may have a higher risk of metastasis (2,10).

As is well known, biliary injury is a direct cause of the formation of biloma (25-27). Sakamoto *et al* (28) found that the incidence of intrahepatic biloma formation in patients with a metastatic liver tumor was higher than that in patients with hepatocellular carcinoma. In the present patient, a biloma, measuring 8x6 cm, was found inside the ALK-negative IMT. We hypothesized that in this case, the formation of the biloma was associated with the lack of expression of the ALK gene and the formation of the *ETV6-NTRK3* fusion gene.

To the best of our knowledge, this is the first report of a case of ALK-negative hepatic IMT harboring the *ETV6-NTRK3* fusion gene and manifesting with biloma. However, the underlying mechanism of this disease remains unclear. von der Thüsen *et al* (29) found that the *ETV6-NTRK3* fusion gene encodes an activated membrane receptor kinase protein, which can promote cell proliferation and survival through the activation of the Ras-MAP kinase and PI3K-Akt pathways. The *ETV6-NTRK3* fusion gene is also associated with secretory carcinoma (30,31). Tang *et al* (32) reported a case of secretory carcinoma of the breast harboring the *ETV6-NTRK3* fusion gene, which showed chemo-resistance to neoadjuvant chemotherapy and multiple distant metastases. Accordingly, we hypothesize that the ALK-negative hepatic IMT with an *ETV6-NTRK3* fusion gene in the present case was significantly more likely to invade and damage the biliary tract, which eventually led to the formation of the biloma. As no similar cases have been reported in the past, it remains uncertain as to whether this is a significant observation, and further research will be required to illuminate the mechanism of this disease.

In conclusion, the present case is of particular interest for two reasons. First, it is not a typical case of hepatic IMT owing to the ALK-negativity of the tumor upon immunohistochemistry and FISH, as well as the presence of an *ETV6-NTRK3* fusion. Secondly, the report provides the first demonstration of a biloma in an ALK-negative IMT of the liver.

Acknowledgements

Not applicable.

Funding

No funding was received.

Authors' contributions

KH and JY designed the study and wrote the manuscript. PWZ, JYZ, PZ and KH performed all the experiments. JY, PWZ and KH confirm the authenticity of all the raw data. All authors read and approved the final version of the manuscript.

Ethics approval and consent to participate

This study has been approved by The Mianyang Hospital of Traditional Chinese Medicine (Mianyang, China; approval number, 2020LL-12). Written informed consent was obtained.

Patient consent for publication

Written informed consent for publication was obtained.

Competing interests

The authors declare that they have no competing interests.

References

1. Zhou P, Chen YH, Lu JH, Jin CC, Xu XH and Gong XH: Inflammatory myofibroblastic tumor after breast prosthesis: A case report and literature review. World J Clin Cases 10: 1432-1440, 2022.
2. Zhang GH, Guo XY, Liang GZ and Wang Q: Kidney inflammatory myofibroblastic tumor masquerading as metastatic malignancy: A case report and literature review. World J Clin Cases 7: 4366-4376, 2019.
3. Thompson LDR: Inflammatory myofibroblastic tumor. Ear Nose Throat J 100 (5_suppl): 520S-521S, 2021.
4. Takahashi A, Kurosawa M, Uemura M, Kitazawa J and Hayashi Y: Anaplastic lymphoma kinase-negative uterine inflammatory myofibroblastic tumor containing the ETV6-NTRK3 fusion gene: A case report. J Int Med Res 46: 3498-3503, 2018.
5. Beauchamp A, Villanueva A, Feliciano W and Reymunde A: Inflammatory myofibroblastic tumor of the liver in an elderly woman following a second liver biopsy: A case report. Bol Asoc Med P R 103: 60-64, 2011.
6. Zhang Y, Zheng G, Meng X, Li Y, Shi D and Yu J: Microwave ablation for the management of pulmonary inflammatory myofibroblastic tumor: A case report and literature review. Transl Cancer Res 10: 4582-4590, 2021.
7. Zhao HD, Wu T, Wang JQ, Zhang WD, He XL, Bao GQ, Li Y, Gong L and Wang Q: Primary inflammatory myofibroblastic tumor of the breast with rapid recurrence and metastasis: A case report. Oncol Lett 5: 97-100, 2013.
8. Tang Z, Li C, Kang B, Gao G, Li C and Zhang Z: GEPIA: A web server for cancer and normal gene expression profiling and interactive analyses. Nucleic Acids Res 45: W98-W102, 2017.
9. Mariño-Enríquez A, Wang WL, Roy A, Lopez-Terrada D, Lazar AJ, Fletcher CD, Coffin CM and Hornick JL: Epithelioid inflammatory myofibroblastic sarcoma: An aggressive intra-abdominal variant of inflammatory myofibroblastic tumor with nuclear membrane or perinuclear ALK. Am J Surg Pathol 35: 135-144, 2011.
10. Yamamoto H, Yoshida A, Taguchi K, Kohashi K, Hatanaka Y, Yamashita A, Mori D and Oda Y: ALK, ROS1 and NTRK3 gene rearrangements in inflammatory myofibroblastic tumours. Histopathology 69: 72-83, 2016.
11. Alassiri AH, Ali RH, Shen Y, Lum A, Strahlendorf C, Deyell R, Rassekh R, Sorensen PH, Laskin J, Marra M, *et al*: ETV6-NTRK3 is expressed in a subset of ALK-Negative inflammatory myofibroblastic tumors. Am J Surg Pathol 40: 1051-1061, 2016.
12. Balfour J and Ewing A: Hepatic Biloma. In: StatPearls [Internet]. Treasure Island (FL) StatPearls Publishing, 2022 Jan 2021.
13. FaisalUddin M, Bansal R, Iftikhar PM, Khan J and Arastu AH: A rare case report of biloma after cholecystectomy. Cureus 11: e5459, 2019.

14. Jo VY and Fletcher CD: WHO classification of soft tissue tumours: An update based on the 2013 (4th) edition. Pathology 46: 95-104, 2014.
15. Coffin CM, Watterson J, Priest JR and Dehner LP: Extrapulmonary inflammatory myofibroblastic tumor (inflammatory pseudotumor). A clinicopathologic and immunohistochemical study of 84 cases. Am J Surg Pathol 19: 859-872, 1995.
16. Shukla PS and Mittal K: Inflammatory myofibroblastic tumor in female genital tract. Arch Pathol Lab Med 143: 122-129, 2019.
17. Zhao JJ, Ling JQ, Fang Y, Gao XD, Shu P, Shen KT, Qin J, Sun YH and Qin XY: Intra-abdominal inflammatory myofibroblastic tumor: Spontaneous regression. World J Gastroenterol 20: 13625-13631, 2014.
18. Kim SH, Cho YH and Kim HY: Two cases of infantile intra-abdominal inflammatory myofibroblastic tumor. Pediatr Gastroenterol Hepatol Nutr 17: 116-120, 2014.
19. Koirala R, Shakya VC, Agrawal CS, Khaniya S, Pandey SR, Adhikary S and Pathania OP: Retroperitoneal inflammatory myofibroblastic tumor. Am J Surg 199: e17-19, 2010.
20. Corapçioğlu F, Kargi A, Olgun N, Ozer E, Olguner M and Sarialioğlu F: Inflammatory myofibroblastic tumor of the ileocecal mesentery mimicking abdominal lymphoma in childhood: Report of two cases. Surg Today 35: 687-691, 2005.
21. Nakamura Y, Inui K, Yoshino J, Tokoro T, Sabater L, Takeda S, Yamashita K, Okochi O and Nakao A: Inflammatory myofibroblastic tumor (inflammatory fibrosarcoma) of the pancreas: A case report. Hepatogastroenterology 52: 625-628, 2005.
22. Morris SW, Kirstein MN, Valentine MB, Dittmer KG, Shapiro DN, Saltman DL and Look AT: Fusion of a kinase gene, ALK, to a nucleolar protein gene, NPM, in non-Hodgkin's lymphoma. Science 263: 1281-1284, 1994.
23. Coffin CM, Patel A, Perkins S, Elenitoba-Johnson KS, Perlman E and Griffin CA: ALK1 and p80 expression and chromosomal rearrangements involving 2p23 in inflammatory myofibroblastic tumor. Mod Pathol 14: 569-576, 2001.
24. Lovly CM, Gupta A, Lipson D, Otto G, Brennan T, Chung CT, Borinstein SC, Ross JS, Stephens PJ, Miller VA and Coffin CM: Inflammatory myofibroblastic tumors harbor multiple potentially actionable kinase fusions. Cancer Discov 4: 889-895, 2014.
25. Bhagat N, Reyes DK, Lin M, Kamel I, Pawlik TM, Frangakis C and Geschwind JF: Phase II study of chemoembolization with drug-eluting beads in patients with hepatic neuroendocrine metastases: High incidence of biliary injury. Cardiovasc Intervent Radiol 36: 449-459, 2013.
26. Suzuki K, Hashimoto T, Osugi S, Toyota N, Omagari K and Tamura A: Spontaneous biloma resulting from intrahepatic bile duct perforation coexisting with intrahepatic cholelithiasis and cholangiocarcinoma: A case report and literature review. Am J Case Rep 21: e926270, 2020.
27. Stonelake S, Ali S, Pinkey B, Ong E, Anbarasan R, McGuirk S, Perera T, Mirza D, Muiesan P and Sharif K: Fifteen-year single-center experience of biliary complications in liver trauma patients: Changes in the management of posttraumatic bile leak. Eur J Pediatr Surg 31: 245-251, 2021.
28. Sakamoto I, Iwanaga S, Nagaoki K, Matsuoka Y, Ashizawa K, Uetani M, Fukuda T, Okimoto T, Okudaira S, Omagari K, *et al*: Intrahepatic biloma formation (bile duct necrosis) after transcatheter arterial chemoembolization. AJR Am J Roentgenol 181: 79-87, 2003.
29. von der Thüsen JH, Dumoulin DW, Maat APWM, Wolf J, Sadeghi AH, Aerts JGJV and Cornelissen R: ETV6-NTRK3 translocation-associated low-grade mucinous bronchial adenocarcinoma: A novel bronchial salivary gland-type non-small cell lung cancer subtype. Lung Cancer 156: 72-75, 2021.
30. Laé M, Fréneaux P, Sastre-Garau X, Chouchane O, Sigal-Zafrani B and Vincent-Salomon A: Secretory breast carcinomas with ETV6-NTRK3 fusion gene belong to the basal-like carcinoma spectrum. Mod Pathol 22: 291-298, 2009.
31. Osako T, Takeuchi K, Horii R, Iwase T and Akiyama F: Secretory carcinoma of the breast and its histopathological mimics: Value of markers for differential diagnosis. Histopathology 63: 509-519, 2013.
32. Tang H, Zhong L, Jiang H, Zhang Y, Liang G, Chen G and Xie G: Secretory carcinoma of the breast with multiple distant metastases in the brain and unfavorable prognosis: A case report and literature review. Diagn Pathol 16: 56, 2021.